Available online at www.sciencedirect.com
ScienceDirect
Polymer 48 (2007) 2231–2240
polymer
www.elsevier.com/locate/polymer

A comparative study of UV active silane-grafted and ion-exchanged organo-clay for application in photocurable urethane acrylate nano- and micro-composites

Katherine M. Dean, Stuart A. Bateman*, Ranya Simons

CSIRO Manufacturing and Materials Technology, 37 Graham Road, Highett, Victoria 3190, Australia

Received 11 September 2006; received in revised form 6 February 2007; accepted 15 February 2007
Available online 20 February 2007

Abstract

A number of urethane acrylate nano- and micro-composites have been developed using both ion exchange and silane grafting chemistry. The organically modified clays which were used contained either methacrylate or acrylate functionalities which were capable of reacting with the acrylate groups in the urethane acrylate matrix. [2-(Acryloyloxy)ethyl]trimethyl-ammonium ion (AOETMA) or [2-(methacryloyloxy)ethyl]trimethylammonium ion (MAOTMA) were exchanged onto montmorillonite (MMT) as shown by an increase in the inter-gallery spacing of the MMT. Silane grafting was undertaken using [3-(acryloxy)propyl]dimethylmethoxysilane (APDMMS) or [3-(methacryloxy)propyl]dimethylmethoxysilane (MAPDMMS) and also showed an increase in inter-gallery spacing. The structures of the resulting urethane acrylate composites were characterized using X-ray diffraction (XRD) and transmission electron microscopy (TEM) and showed predominantly intercalated structures with some exfoliation (more evident in the silane-grafted systems). Dynamical mechanical thermal analysis (DMTA) showed a more significant increase in effective crosslink density (as measured from the plateau of the rubbery modulus) in the composites containing the reactive clays as compared to the unmodified clay, supporting the concept that the acrylate and methacrylate functionalities of the modified clays had reacted with the matrix. Other thermal and mechanical properties were also evaluated.

Keywords: Urethane acrylate; Nanocomposite; UV curing

1. Introduction

Photo-induced polymerization is a well-documented technique for the rapid and precise formation of crosslinked polymers from liquid monomers [1–4] and has numerous uses in the medical and coating industries [3–5]. A significant body of work has been undertaken on the free radical polymerization of acrylate-based resins, due to their high reactivity and broad ranges of backbone chemistries (and thus properties). They have been used extensively in both thermal-initiated and photo-initiated applications [3]. Within the acrylate family, urethane acrylates have unique properties such as high flexibility, toughness and chemical resistivity, as such are widely used in the coating industry [4,6–8]. Due to their high viscosities urethane acrylate is usually blended with reactive diluents such as short chain monoacrylates to reduce viscosity and also to modify crosslink density [9].

The inclusion of nanoclays and nanoparticles has been utilized in many photocured acrylate and methacrylate systems [10–14]. A number of authors have reported improvements in physical properties with the inclusion of the typical alkyl ammounium modified nanoclays generally without significant changes to the polymerization kinetics of the acrylate or methacrylate itself [10–12]. Solomon and Swift suggested more complicated interactions between nanoclays and free radical polymerizations; the introduction of high surface area clays

* Corresponding author. Tel.: +613 9252 6000; fax: +613 9252 6244.
E-mail address: stuart.bateman@csiro.au (S.A. Bateman).

0032-3861/$ - see front matter Crown Copyright © 2007 Published by Elsevier Ltd. All rights reserved.
doi:10.1016/j.polymer.2007.02.044

can reduce the radical concentration by surface collisions and/or the aluminium ion at the nanoclays edge can act as an electron accepting site, absorbing the propagating free radical causing oxidation of the free radicals to carbonium ions or termination by combination or disproportionation [15].

Other authors have investigated the effects modifying nanoclays with the ion exchange of a reactive organic ion, in which a vinyl, acrylate or methacrylate functionality on the modified clay can react with the acrylate or methacrylate matrix [13,14,16,17]. Yebassa et al. studied the effect of the inclusion of a non-reactive and reactive modified clay in a thermally-cured vinyl ester matrix and found that ion exchange of the reactive onium salt (ω-undecylenyl amine hydrochloride) and the non-reactive onium ion (undecyl amine hydrochloride) increased the gallery spacing to 0.42 and 0.41 nm, respectively [13]. When these clays were dispersed in a vinyl ester resin using processing aids such as ultrasonics the reactive modified clay appeared to produce the highest degree of exfoliation as observed by using TEM.

Fu and Qutubuddin studied the effect of the dispersion of two different vinyl modified clays in a thermally-cured polyester matrix. The vinylbenzyldodecyldimethyl ammonium modified montmorillonite polyester system produced an intercalated nanocomposite while the vinylbenzyloctadecyldimethyl ammonium modified montmorillonite polyester system formed partially exfoliated nanocomposites, possibly due to the longer alkyl chain in the latter leading to greater initial platelet separation in the nanoclay itself [16,17].

Keller et al. also dispersed non-reactive alky modified nanoclays and reactive acrylate modified nanoclays into acrylate-based matrices (in this case a photopolymerised urethane acrylate). XRD spectra showed an expansion of the inter-gallery spacing upon organo-treatment with the non-reactive alkyl modified clay and a decrease in intensity of the d_{001} peak in the nanocomposite indicating a high level of exfoliation. The reactive acrylate modified clays were also dispersed in the urethane acrylate matrix, although dispersion information was not reported, the inclusion of the reactive modified clays did not affect the conversion of the C=C in the urethane acrylate matrix and no significant improvement in modulus or increase in T_g was observed [14].

Uhl et al. also studied the effect of modified montmorillonites in photocurable urethane acrylate systems. Cetyltrimethylammonium bromide (CTMA) and [(2-acryloyloxy)ethyl](4-benzoyl-benzyl)dimethylammonium bromide (AEBBDMA) were exchanged onto montmorillonite as shown by an expansion of inter-gallery spacing using XRD and by thermal gravimetric analysis. Intercalated and exfoliated structures were observed and thermal and mechanical properties were generally improved with nanoclay reinforcements [18].

Modification of nanoclays and nanoparticles to make them organophilic and hence more compatible with the polymer matrix can also be undertaken using silane grafting to the edge hydroxyl groups on clay or particle [19–23]. Wheeler et al. grafted up to 14% of both mono- and tri-functional alkoxy silanes to laponite clays [19]. He et al. also grafted silane to the surfaces of nanoclays (naturally occurring montmorillonite and a synthetic fluorohectorite) as shown by an expansion of the inter-gallery spacing of the clays and the presence of the CH_2 from the silane in infra-red spectroscopy of the modified clays [20].

In this study we prepare four modified clays using both ion exchange and silane grafting chemistry, producing UV active clays containing either acrylate or methacrylate functionalities capable of reacting with the acrylate groups of the urethane acrylate matrix itself. The resulting properties of both clays and resulting nano- and micro-composites and related physical and chemical aspects of their morphologies are discussed in detail.

2. Experimental

2.1. Materials

The urethane acrylate used was an aliphatic urethane acrylate (UA, CN966 supplied by Sartomer); 30 wt% isobornyl acrylate (IA) was used as a reactive diluent; 1 wt% acylphosphine oxide (Irgacure 819 supplied by Ciba Specialty Chemicals, see Fig. 1A) was used as the photoinitiator for photocuring using ultraviolet radiation. The fast photo-bleaching of the strongly absorbing acylphosphine oxide photoinitiator makes the incident radiation penetrate progressively further into the sample, thus promoting a frontal polymerization process [24].

Different modified and unmodified montmorillonite clays were used in this study. The unmodified sodium montmorillonite (Na-MMT) and conventionally modified montmorillonite (methyl, tallow, bis-2-hydroxyethyl ammonium ion, Cloisite 30B, see Fig. 1B) were supplied by Southern Clay Products and were used as received. The two ion exchanges

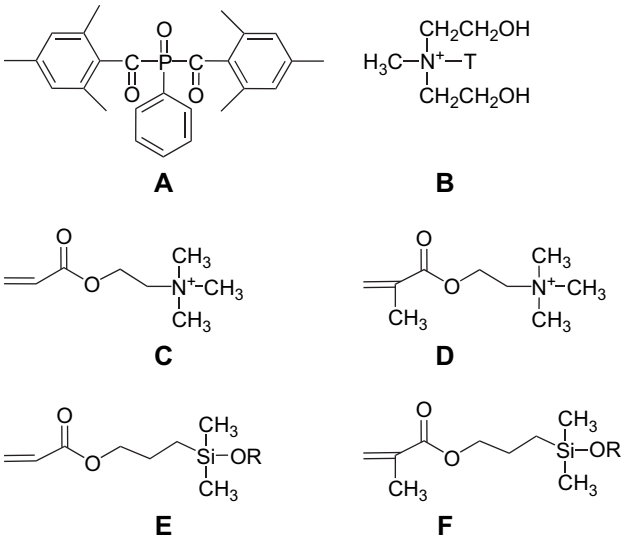

Fig. 1. Chemical structures of: A, UV initiator acylphosphine oxide – Irgacure 819 and clay modification reagents; B, methyl, tallow, bis-2-hydroxyethyl ammonium ion (T is tallow 65 wt% C18, 30 wt% C16, 5 wt% C14); C, [2-(acryloyloxy)ethyl]trimethyl-ammonium ion (AOETMA); D, [2-(methacryloyloxy)-ethyl]trimethylammonium ion (MAOTMA); E, [3-(acryloxy)propyl]dimethylmethoxysilane (APDMMS); F, [3-(methacryloxy)propyl]dimethylmethoxysilane (MAPDMMS).

were undertaken using either the [2-(acryloyloxy)ethyl]trimethyl-ammonium ion (AOETMA) or [2-(methacryloyloxy)-ethyl]trimethylammonium ion (MAOTMA) (both supplied by Aldrich, see Fig. 1C and D, respectively). Silane grafting was undertaken using [3-(acryloxy)propyl]dimethylmethoxysilane (APDMMS) or [3-(methacryloxy)propyl]dimethylmethoxysilane (MAPDMMS) (supplied by Gelest, see Fig. 1E and F, respectively). Alkyl ammonium ions and silanes were all inhibited with approximately 500 ppm monomethyl ether hydroquinone (MEHQ).

2.2. Clay modification

2.2.1. Ion exchange

Na-MMT (cation exchange capacity (CEC) = 92 meq/100 g) was suspended in 70 °C distilled water (20 g Na-MMT/3 L water) and stirred for 1 h. A 10% excess of AOETMA was then added to the solution and the resultant suspension was stirred at heat for a further 1 h. The resulting suspension was filtered and washed repeatedly with warm distilled water until no chloride ions were detected using 0.1 M $AgNO_3$ solution. The resulting modified clay was preliminarily dried (75 °C) for 12 h. The resultant granular organically modified clay was ground to a particle size of less than 45 μm and then further dried at 75 °C prior to processing or analysis. A similar procedure was used for the preparation of MAOTMA exchange with Na-MMT.

2.2.2. Silane grafting

Na-MMT was suspended in 70 °C de-ionized water:ethanol (75:25 vol%) solution (20 g Na-MMT/3 L solution) and stirred for 1 h. An excess of APDMMS was added separately to 1 L of a 75:25 vol% solution of de-ionized water:ethanol (pH adjusted to 4 using acetic acid) and stirred for 1 h. The solutions were combined at ambient temperatures and stirred for 5 days at this temperature (the silane grafting procedure was adopted from techniques reported previously [20]) [25]. The modified clay was filtered using vacuum filtration and washed repeatedly in a 75:25 vol% de-ionized water:ethanol solution to remove any free APDMMS. The precipitate was then preliminarily dried (75 °C) for 12 h. The resultant granular organically modified clay was ground to a particle size of less than 45 μm and then further dried at 75 °C prior to processing or analysis. A similar procedure was used for the preparation of MAPDMMS grafted Na-MMT.

2.3. Photopolymerisation

The liquid resin together with the photo-initiation system was heated to 70 °C and stirred constantly for 20 min to allow the Irgacure 819 to dissolve. At all times samples were not exposed to light (either natural or artificial) to minimise the likelihood of premature polymerization. Modified clays were first dispersed in the low viscosity isobornyl acrylate. The isobornyl acrylate/clay solution was then blended into the higher viscosity urethane acrylate system placed in a heated (60 °C) ultrasonic bath for 5 h. After all components in each system were dissolved completely the samples were de-gassed under vacuum to remove entrapped air. The resin was injected into a mould formed by a 1 mm thick silicone gasket (width 20 mm, length 150 mm), sandwiched between two glass slides and PET release films to allow easy removal of the sample.

A Fusion curing unit was used for the ultraviolet light photopolymerisation of the urethane acrylate systems. This bulb in this unit had a dominant emittance at 365 nm corresponding to the excitation wavelength of the Irgacure 819. A shutter was used to allow an accurate control of the exposure time of the sample by the light source. Samples were exposed to the UV lamp for a total time of 2 min (1 min on each side).

2.4. Characterization of organo-clays and UV cured urethane acrylate nano- and micro-composites

A Bruker Fourier Transform Infrared Spectrometer (FTIR) was used to observe the chemical modification of the clay at a resolution of 4 cm^{-1}. Clay was ground into KBr powder and pressed into discs prior to being placed in the FTIR for scanning.

Near infra-red spectroscopy (NIR) was used to measure the degree of cure of 1 mm plate samples using the same Bruker FTIR at a resolution of 4 cm^{-1}. The characteristic peaks in the near infra-red region for the acrylate and methacrylate unsaturation occur at 6166 cm^{-1}. A linear fit was used as an approximation of the ''fully cured'' sample and this approximation was subtracted from the NIR spectra. The area under these peaks was used to calculate the conversion of the C=C groups in the uncured and fully cured systems.

^{13}C NMR spectra were observed at room temperature using a Varian Unity plus spectrometer at resonance frequencies of 75 MHz for ^{13}C and 300 MHz for ^{1}H with cross-polarization, magic angle spinning and high power dipolar decoupling (CP/MAS/DD) techniques. The contact time was 1 ms and the 90° pulse was 4.5 μs for ^{1}H and ^{13}C while the spinning rate of MAS was set at a value in the range of 6–7 kHz. The chemical shift of ^{13}C CP/MAS spectra was determined by taking the carbonyl carbon of solid glycine (176.03 ppm) as an external reference standard.

X-ray diffraction (XRD) was performed on a Phillips PW 1729, $CuK_{\alpha 1}$ source $\lambda = 0.154$ nm. For XRD of the nanoclays approximately 3 g of clay was pressed into a sample holder and placed in the diffractometer. For the nanocomposites themselves a 1 mm thick polymer sample was prepared via photopolymerisation, fitted to the sample holder and placed in the diffractometer for scanning.

Thermal gravimetric analysis (TGA) was performed on both the clays and the resulting nanocomposites using a Perkin Elmer-7 TGA; 5–8 mg of sample was heated from 50 °C to 800 °C using a scan rate of 10 °C/min.

Seventy to ninety-nanometer sections of the samples were microtomed at −80 to −100 °C using an Ultracut E microtome at a cutting speed of 0.05 mm/s. A Jeol 100S TEM was used at 100 keV to study dispersions of clay particles TEM.

The dynamic mechanical behaviour of the cured samples was measured at 1 Hz using a Pyris Diamond dynamical mechanical analyzer (DMA) using rectangular samples in tension. The glass transition temperature (T_g) was determined at the maximum tan δ in the dynamic mechanical thermal analysis spectrum at 1 Hz.

Tensile testing was performed on an Instron 5565 according to ASTM standard D412. Tensile strength, stress and yield point were determined with a rate of grip separation of 250 mm/min. The modulus was determined with a rate of grip separation of 25 mm/min. Tear strength measurements were also performed using an Instron 5565 Universal Testing Apparatus according to ASTM D624 Type T employing a grip separation rate of 50 mm/min.

3. Results and discussion

3.1. Clay modification

The various organo-modified nanoclays studied in this work were characterized using XRD, FTIR, ^{13}C NMR and TGA, to confirm both qualitatively and quantitatively the grafting or exchanging of the reactive organo-groups to the clay surfaces, edges or within inter-gallery spacing. FTIR spectra of both the ion-exchanged and silane-grafted clays are shown in Fig. 2, with characteristic peaks of both the organic modification and the silicates themselves summarized in Table 1.

The C═C group present in acrylates and methacrylates has characteristic peaks at 1640 cm^{-1} [26], 945 cm^{-1} [27] and 1410 cm^{-1} [11]. A number of characteristic peaks for the silicate are also present in the FTIR spectra. Due to overlapping of these peaks the peak at 1410 cm^{-1} was used to indicate the presence of C═C in the modified clays.

The d_{001} spacings for the Na-MMT and modified clays were obtained using XRD and are summarized in Table 2. It can be seen that the ion-exchanging and silane grafting of organo-component increase the d_{001} spacing of the clays. Both ion-exchanged clays (AOETMA-MMT and MAOTMA-MMT) increased in basal spacing by 2.4 Å, whereas the silane-grafted systems increased by 4.4 Å and 5.8 Å for the APDMMS-MMT and MAPDMMS-MMT, respectively.

Table 1
Characteristic FTIR peaks for MMT modification

Group		Wavenumber (cm^{-1})
Organic	C═C	945, 1410, 1640 [11,26]
	C═O	1720
Silicate	Framework OH stretch	3631 [28]
	Interlayer H_2O stretch	3428 [28]
	H–O–H def	1643 [28]
	Al–Al–OH stretching in octahedral layer	932 [28]

The greater expansion in inter-gallery spacing realized by the silane grafting strategy and hence extent of organo-modification was also supported by TGA (see Fig. 3) since a larger weight percentage of organic functionality was associated with the clay surface as compared to the ion-exchange method. The as received Na-MMT contained approximately 9 wt% water and did not undergo any significant weight loss after the removal of water. The modified clays of AOETMA-MMT, MAOTMA-MMT, APDMMS-MMT and MAPDMMS-MMT contained approximately 10 wt%, 17 wt%, 10 wt% and 22 wt% organic component, respectively, as shown by TGA, taking into consideration that stable weight loss up to 100 °C was due to water loss. TGA also confirmed that there was no un-reacted silane present as APDMMS had a boiling point of 70.2 °C and MAPDMMS had a boiling point of 54.5 °C and no significant weight loss was observed at these temperatures. As the silanol group can only react with the edge –OH groups it may be expected that a lower percentage organo-silane would

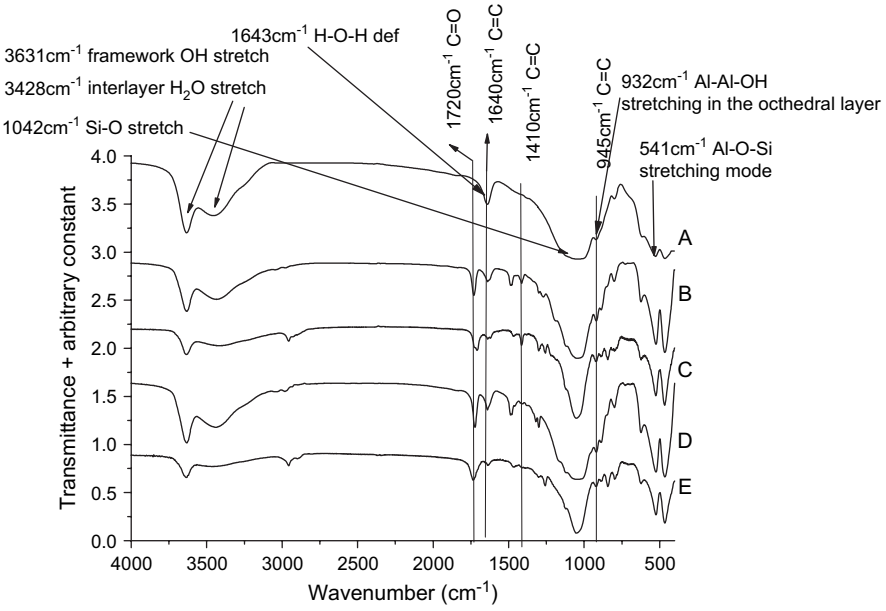

Fig. 2. FTIR of: A, MMT; B, AOETMA-MMT; C, APDMMS-MMT; D, MAOTMA-MMT; E, MAPDMMS-MMT.

Table 2
XRD d_{001} spacings for Na-MMT and organo-modified MMT (modified via ion exchange or silane grafting)

Sample	Basal spacing d_{001} (Å)
Na-MMT	11.7
30B	17.0
AOETMA-MMT	14.1
APDMMS-MMT	16.1
MAOTMA-MMT	14.1
MAPDMMS-MMT	17.5

be present in these modified clays (assuming similar molecular weights of organic component), this discrepancy for the greater d_{001} spacing and higher organic component may be explained by a number of different mechanisms including physical interaction and entrapment between the clay platelets as well as polymerization of the silane precursors prior to or following the grafting reaction.

Although both silanes and ammonium ions were inhibited with MEHQ the longer reaction time employed for the silane grafting (5 days) may have enabled more polymerization of the acrylate or methacrylate double bonds to produce the structures outlined in Fig. 4 and a higher percentage of organic component present (Fig. 4B) as suggested by TGA analysis and noted in the XRD basal spacing results. In this case numerous grafting structures would be possible including a single point of attachment, cyclic structures with two or more points of attachment to one platelet as well as and platelet bridging configurations. Although the polymerization of these double bonds may have been reduced by surface collisions of the radicals with the clay or by the clays acting as radical traps as suggested previously [15]; any polymerization may be further reduced by the addition of inhibitors, removal of all light exposure and manipulation of reaction temperatures.

Reaction is also possible between silanol moieties generated under the grafting conditions not only via the acrylate and methacrylate double bonds. The choice of monoalkoxy silane precursors (as opposed to tri-alkoxy silanes which have

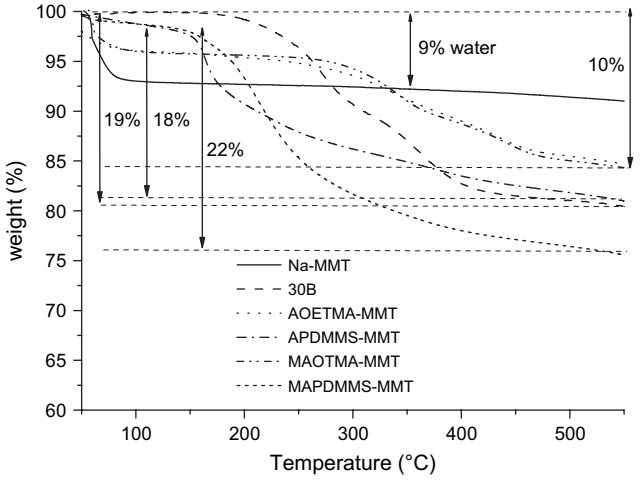

Fig. 3. TGA of Na-MMT and modified clays.

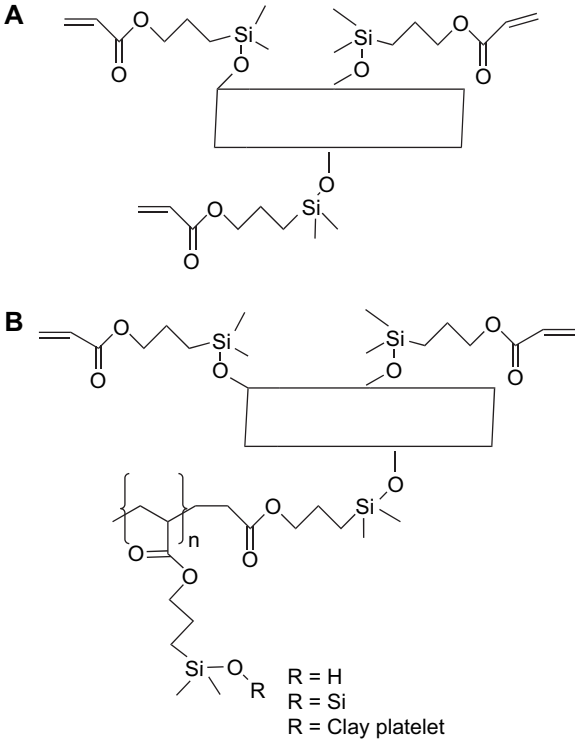

Fig. 4. A: Ideal configuration for silane grafted onto edge hydroxyl groups in montmorillonite; B: possible chain extension configurations for acrylate-based silane grafted onto montmorillonite.

been shown to crosslink around layered silicates in previous work [25]) limited this reaction to non-grafting dimerisation.

The ^{13}C NMR spectra for the four modified clays are shown in Fig. 5. The spectra show peaks at 120 ppm corresponding to the chemical shift for C═C group [29], the presence of this peak is supporting evidence for the FTIR spectra of the modified clays which also show the presence of the C═C group. The broadness of this peak (which stretches from 120 to 165 ppm) may be due to a contribution from the C═O group which has been shown by previous authors to have a shift at 164.5 [13].

3.2. UV cured urethane acrylate nanocomposites

3.2.1. XRD

The XRD results for the nanocomposites containing 5 wt% clay are shown in Fig. 6, and the corresponding inter-gallery spacings (d_{001}) are shown in Table 3. Both ion-exchanged and silane-grafted clays showed higher d_{001} spacing than the unmodified Na-MMT, indicating that the structures were intercalated as the clay platelets were expanded by the matrix. The inter-gallery spacing increased more significantly in the ion-exchanged clays than the silane-grafted clays as seen in Table 3. For the AOETMA-MMT, the spacing increased by 2.3 Å on polymerization, and in the MAOTMA it increased by 1.8 Å while the silane-grafted clays increased by 0.6 and 0.4 Å for the APDMMS-MMT and MAPDMMS-MMT, respectively.

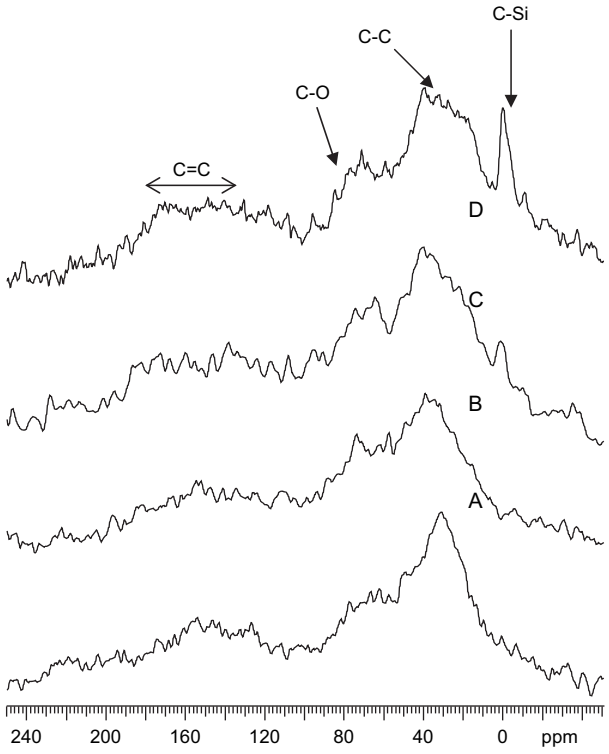

Fig. 5. ^{13}C NMR spectra of: A, AOETMA-MMT; B, MAOTMA-MMT; C, APDMMS-MMT and D, MAPDMMS-MMT.

The silane modified clays (APDMMS-MMT and MAPDMMS-MMT) showed a significant decrease in the intensity of the d_{001} peak in the XRD indicating a loss of platelet order in the system which was later supported by the TEM results (Section 3.2.2). In contrast the ion-exchanged clays (AOETMA-MMT and MAOTMA-MMT) still showed a relatively intense d_{001} peak (shifted to a larger 2θ values), suggesting a level of intercalated clay morphologies.

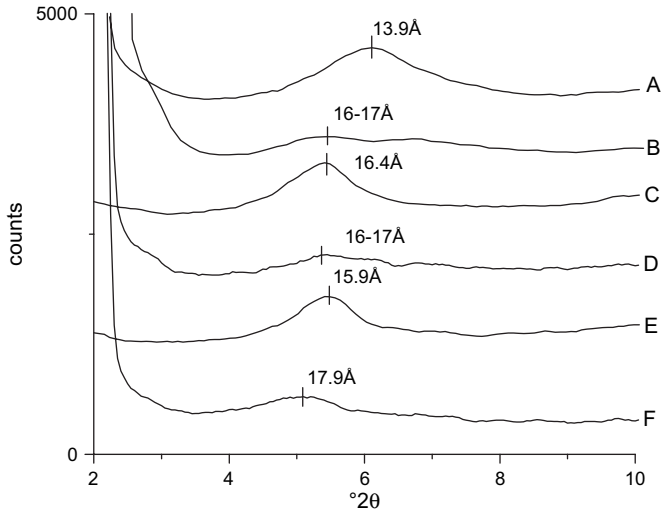

Fig. 6. XRD spectra of: A, 5 wt% Na-MMT nanocomposite; B, 5 wt% 30B; C, 5 wt% AOETMA-MMT nanocomposite; D, 5 wt% APDMMS-MMT nanocomposite; E, 5 wt% MAOTMA-MMT nanocomposite; F, 5 wt% MAPDMMS-MMT nanocomposite.

Table 3
XRD d_{001} spacings for 5% loaded nanocomposites and straight clays

Sample	Inter-gallery spacing d_{001} of 5 wt% composites (Å)	Inter-gallery spacing d_{001} of clays (Å)
Na-MMT	13.9	11.7
30B	16–17	17.0
AOETMA-MMT	16.4	14.1
APDMMS-MMT	16–17	16.1
MAOTMA-MMT	15.9	14.1
MAPDMMS-MMT	17.9	17.5

3.2.2. TEM

TEM images of the 5 wt% Na-MMT, 5 wt% AOETMA-MMT and 5 wt% APDMMS-MMT composites are shown in Fig. 7. Large agglomerates/tactoids are clearly visible in the Na-MMT sample (see Fig. 7A). Large agglomerates/tactoids are also visible in AOETMA-MMT nanocomposites (see Fig. 7B), but this material also had smaller tactoids of 5–10 platelets and some single platelets, indicative of better dispersion as illustrated in reduced intensity of d_{001} peak in XRD spectra. The APDMMS-MMT nanocomposite showed the best dispersion (Fig. 7C), where smaller agglomerates/tactoids in (approximately 10–15% of size c/f Na-MMT) and single tactoids were visible. Similar results were observed in the methacrylate-based systems. It is foreseeable that initial grinding of the modified clays to smaller dimensions prior to dispersion and photopolymerisation would also assist in providing smaller intercalated tactoids and higher levels of disorder (exfoliation) in the systems.

3.2.3. FTIR conversion

Fig. 8 shows the NIR spectra for the uncured urethane acrylate resin and all the resulting composites containing 5 wt% clay. The conversion of C=C as measured by area of the peak at 6163 cm^{-1} reaches 97–98% for all the nanocomposites (see Table 4). The presence of nanoclays (whether unmodified or modified) did not significantly reduce the level of cure in the urethane acrylate matrix under the cure conditions employed. Any inhibition of the urethane acrylate system due to the interactions with the clay [15] was not clearly visible, although this will be discussed in further detail in relation to crosslink density from the DMTA results.

3.2.4. DMTA

The DMTA scans for the neat urethane acrylate and corresponding composites containing 5 wt% clay are shown in Fig. 9. The resulting T_gs, rubbery modulus values and crosslink density (as calculated from the rubbery modulus plateau) are listed in Table 5. In the neat urethane acrylate system two T_gs are observed, the lower temperature T_g (−10 to −20 °C) corresponding to a urethane acrylate-rich phase and the higher temperature T_g corresponding to the dominant urethane acrylate/isobornyl acrylate phase (60–80 °C), similar results were observed by Allen et al. in urethane acrylate systems containing reactive diluents such as methyl acrylate or tetra-(ethylene glycol) diacrylate [9].

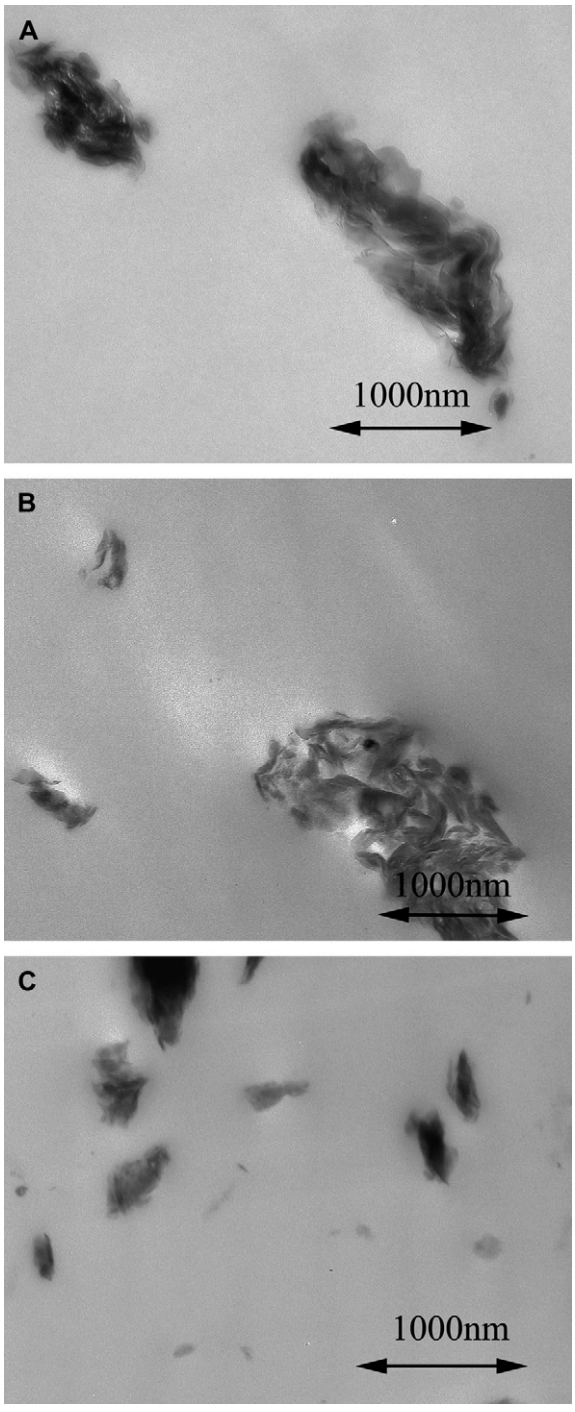

Fig. 7. TEM images of: A, 5 wt% Na-MMT; B, 5 wt% AOETMA-MMT and C, 5 wt% APDMMS-MMT nanocomposites.

The higher temperature T_g due to the minor isobornyl acrylate-rich phase increased upon addition of nanoclays, most significantly for the unmodified Na-MMT. This may be explained by the fact that the various modifications of the nanoclays may have reduced the ability of the isobornyl acrylate to penetrate into the inter-gallery spacings; however, in the unmodified Na-MMT the isobornyl acrylate could migrate into the inter-gallery spacing and remained there, where upon curing could have produced a Na-MMT-rich iosbornyl acrylate phase. The

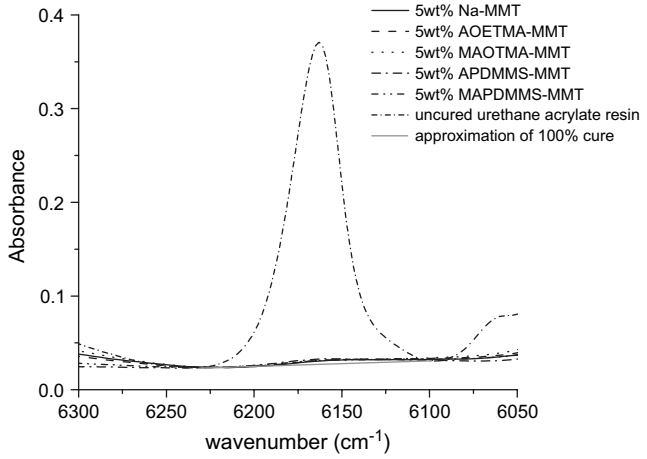

Fig. 8. FTIR spectra for cured urethane acrylate and various nanocomposite systems showing disappearance of C=C absorbance at 6163 cm^{-1}.

sub-ambient T_g of the major urethane acrylate component increased by 1–4 °C as compared to the neat system upon addition of the various nanoclays, and more significantly for the reactively modified clay systems. Further morphological analysis is required, however, these results were shown to be in agreement with the increases in effective crosslink density for the nanocomposite systems which was calculated using the following equation:

$$E = 3\upsilon_e RT \quad (1)$$

where E is modulus, υ_e is the crosslink density, R is the universal gas constant (8.314 J mol^{-1} K^{-1}) and T is the absolute temperature [30].

An increase in effective crosslink density (Table 5) was observed in the systems containing nanoclays (whether modified or unmodified). This is what might be expected from the acrylate or methacrylate functionalized clays, in which it is proposed that the modified clay acts as a crosslinker with the acrylate groups in the resin matrix. The apparent increase in crosslink density for the unmodified clay cannot be explained by this mechanism but may in fact be due to physical aggregation of the polymer chains onto the clay surface as shown in other polymer nanocomposite systems [18].

The acrylate modified clays (both ion-exchanged and silane grafted) produced the two highest effective crosslink densities (AOETMA-MMT 399 mol/m^3 and APDMMS 414 mol/m^3)

Table 4
Conversion of C=C in fully cured samples

	5 wt% Clay	2.5 wt% Clay	1 wt% Clay
Na-MMT	97 ± 2%	98 ± 2%	98 ± 2%
30B[a]	97 ± 2%	97 ± 2%	97 ± 2%
Ion exchanged			
AOETMA-MMT	97 ± 2%	97 ± 2%	98 ± 2%
MAOTMA-MMT	98 ± 2%	97 ± 2%	98 ± 2%
Silane grafted			
APDMMS-MMT	98 ± 2%	97 ± 2%	98 ± 2%
MAPDMMS-MMT	97 ± 2%	98 ± 2%	98 ± 2%

[a] Please note data not shown in Fig. 8.

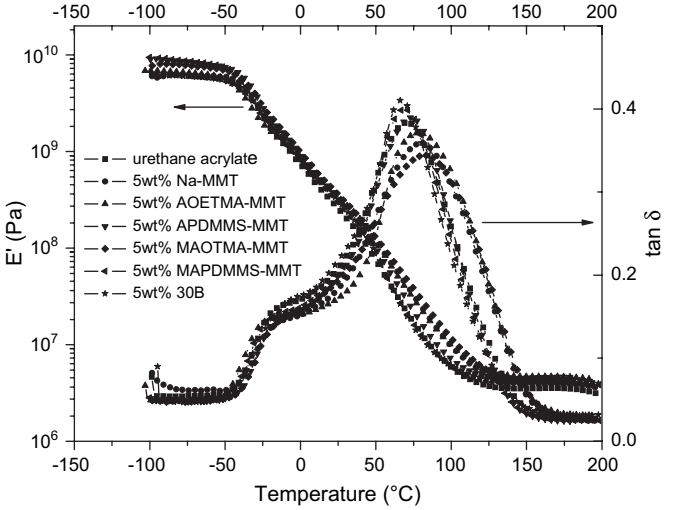

Fig. 9. DMTA of neat urethane acrylate, 5 wt% Na-MMT, 5 wt% AOETMA-MMT, 5 wt% APDMMS-MMT, 5 wt% MAOTMA-MMT and 5 wt% MAPDMMS-MMT nanocomposites.

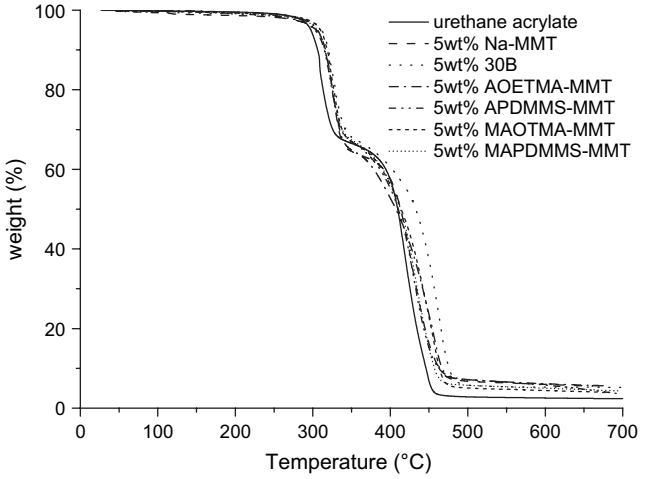

Fig. 10. TGA of neat urethane acrylate, 5 wt% Na-MMT, 5 wt% AOETMA-MMT, 5 wt% APDMMS-MMT, 5 wt% MAOTMA-MMT and 5 wt% MAPDMMS-MMT nanocomposites.

possibly because polyacrylate radicals generally have a higher reactivity than methacrylate radicals [31]. The silane-grafted acrylate system provided the highest effective crosslink density (414 mol/m^3), an effect of (i) greater levels of exfoliation as indicated by TEM analysis, (ii) the reactivity of the acrylate radical and (iii) silane grafting on the clay edges potentially blocking absorption of radicals by edge aluminium ions which has previously been shown to cause termination [15].

3.2.5. TGA

Fig. 10 provides the TGA results for the neat resin and the five corresponding micro- and nano-composites containing 5 wt% of the various clays (both unmodified and modified). The addition of any type of clay increased the onset temperature for the major thermal decomposition phase in the urethane acrylate from ~290 °C to ~310 °C. There is little difference between the unmodified MMT and all the modified clays giving a strong indication that the ion exchange or silane grafting of a reactive acrylate or methacrylate functionality onto the clay does not make the resultant nanocomposite more susceptible to thermal degradation.

3.2.6. Tensile/flexural properties

The modulus and stress at yield increased relatively consistently with increasing amounts of both the modified and unmodified clays (Table 6). The reactive clays did not offer significant improvements in modulus or stress at yield over the Na-MMT but experienced a significantly higher strain at break, indicative of interaction between the grafted acrylate or methacrylate groups and urethane acrylate matrix itself. It should be noted that the 30B did not provide improvements in modulus compared with the virgin matrix unlike all other modified samples. From TGA the organic component of the modified clays was 10%, 17%, 10% and 22% for the AOETMA-MMT, APDMMS-MMT, MAOTMA-MMT and MAPDMMS-MMT, respectively; if this is taken into account in comparing the mechanical properties of the clays (i.e. the clays are compared per equal weight of silicate) the modified clays out perform the Na-MMT by 10–20% for modulus and stress at yield and the silane-grafted clays are between 7 and 12% higher in modulus and stress at break than the ion-exchanged clays.

Table 5
DMTA data

Sample	tan δ peaks	Rubbery E' (Pa)	υ_e (mol/m^3)
Urethane acrylate	−16, 70	3.53×10^6	316
5 wt% Na-MMT	−16, 78	3.92×10^6	351
5 wt% 30B	−15, 67	4.10×10^6	367
5 wt% AOETMA-MMT	−15, 76	4.46×10^6	399
5 wt% APDMMS-MMT	−12, 73	4.63×10^6	414
5 wt% MAOTMA-MMT	−12, 73	4.17×10^6	373
5 wt% MAPDMMS-MMT	−14, 71	4.12×10^6	369

The tear strength for the neat urethane acrylate and corresponding composites containing 2.5 wt% clay is shown in Fig. 11. The higher tear strength recorded for the AOETMA-MMT (1.50 kN/m) and APDMMS-MMT (1.55k N/m) based nanocomposites was possibly due to their greater effective crosslink densities (as measured by DMTA) as compared with the others. On the other hand the methacrylate-based clays (MAOTMA-MMT and MAPDMMS-MMT) had lower tear strengths of 1.46 kN/m and 1.42 kN/m, respectively, possible due to the reduction in crosslink density due to the reduced reactivity of the methacrylate radical as compared with the acrylate radical as mentioned previously [31]. The silane-grafted acrylate system had the best tear strength (1.55 kN/m) as a result of its high effective crosslink density (414 mol/m^3), a result of both the dispersion, reactivity of the acrylate radical and the silane grafting on the clay edge blocking the absorption of the radical by the edge aluminium ion which had previously been shown to cause termination [15]. All acrylate- and methacrylate-based clay systems produced greater increases in tear strength (as compared to their un-reactive counterparts) giving further confirmation that the

Table 6
Mechanical properties

	Percentage of nanoclay	Young's modulus (MPa)	Stress at yield (2% offset) (MPa)	Strain at break (%)
Cured urethane acrylate resin	0	23.6 (0.7)	2.5 (0.1)	217.6 (23.7)
Na-MMT	5	26.2 (3.1)	2.8 (0.3)	217.6 (29.4)
	2.5	22.5 (0.9)	2.9 (0.7)	320.0 (48.0)
	1	21.1 (0.7)	2.6 (0.3)	291.3 (17.4)
30B	5	22.5 (0.7)	2.8 (0.3)	252.3 (25.6)
	2.5	21.8 (0.8)	2.7 (0.3)	324.5 (58.0)
	1	18.4 (1.0)	2.2 (0.1)	322.6 (11.0)
AOETMA-MMT	5	26.8 (2.1)	3.2 (0.1)	244.1 (12.8)
	2.5	25.7 (0.6)	3.1 (0.2)	288.7 (42.6)
	1	21.7 (3.2)	3.1 (0.2)	281.4 (48.0)
APDMMS-MMT	5	26.4 (1.5)	2.8 (0.2)	274.7 (15.2)
	2.5	23.5 (5.0)	3.1 (0.2)	283.4 (30.2)
	1	20.8 (1.7)	2.9 (0.4)	324.1 (46.3)
MAOTMA-MMT	5	27.4 (3.5)	2.8 (0.2)	283.8 (23.4)
	2.5	25.2 (1.5)	2.6 (0.3)	275.6 (32.0)
	1	20.1 (2.2)	2.3 (0.2)	282.0 (34.9)
MAPDMMS-MMT	5	26.6 (1.8)	2.9 (0.3)	272.4 (31.2)
	2.5	26.7 (3.6)	3.0 (0.3)	301.5 (20.1)
	1	21.6 (1.8)	2.3 (0.2)	333.8 (24.9)

Standard deviation listed in parenthesis.

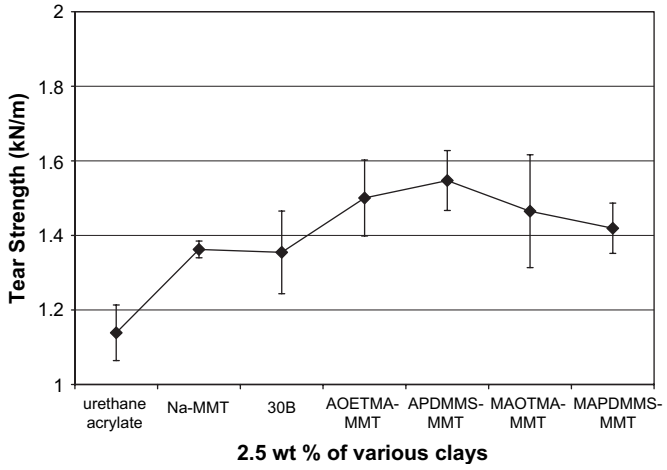

Fig. 11. Tear strength for neat urethane acrylate, 2.5 wt% Na-MMT, 2.5 wt% 30B, 2.5 wt% AOETMA-MMT, 2.5 wt% APDMMS-MMT, 2.5 wt% MAOTMA-MMT and 2.5 wt% MAPDMMS-MMT nanocomposites.

reactive clays had in fact crosslinked into the urethane acrylate matrix.

4. Conclusion

A number of urethane acrylate nano- and micro-composites have been developed using both ion exchange and silane grafting chemistry. The organically modified clays synthesized contained either methacrylate or acrylate functionalities which were capable of reacting with the acrylate groups in the urethane acrylate matrix. AOETMA and MAOTMA were exchanged onto montmorillonite (MMT) as shown by an increase in the inter-gallery spacing of the MMT and via FTIR, NMR and TGA. Silane grafting was undertaken using APDMMS and MAPDMMS and also showed an increase in inter-gallery spacing. The grafting of silane was also confirmed using FTIR, NMR and TGA. The structures of the resulting urethane acrylate micro- and nano-composites were characterized using X-ray diffraction (XRD) and transmission electron microscopy (TEM) and showed predominantly intercalated structures with some exfoliation (more evident in the silane-grafted systems). Dynamical mechanical thermal analysis (DMTA) showed a more significant increase in effective crosslink density (as measured from the plateau of the rubbery modulus) in the composites containing the reactive clays as compared to the Na-MMT, supporting the concept that the acrylate and methacrylate functionalities of the modified clays had reacted with the matrix. DMTA also showed an increase in the glass transition temperature (T_g) upon addition of nanoclays whether modified or unmodified. The modified clays did not significantly improve the modulus or stress at break compared to the Na-MMT composite, but experienced a slightly higher strain at break. The tear strength of the modified clays increased considerably, with the silane-grafted acrylate system (APDMMS) showing the highest tear strength (1.55 kN/m (40% increase c/f neat urethane acrylate)) possibly a result of both the increased reactivity of the acrylate radical and the silane grafting on the clay edge blocking the absorption of the radical species producing a higher effective crosslink density.

Acknowledgements

The authors wish to thank Dr Xiaoqing Zhang for taking the ^{13}C NMR measurements.

References

[1] Moad G, Solomon DH. The chemistry of free radical polymerization. Oxford: Elsevier Science Inc; 1995.
[2] Cook WD. Polymer 1992;33:2152–61.
[3] Decker C. Progress in Polymer Science 1996;21(4):593–650.
[4] Andrzejewska E. Progress in Polymer Science 2001;26(4):605–65.
[5] Cook WD. Journal of Polymer Science, Part A: Polymer Chemistry 1993;31:1053–67.
[6] Assumption HJ, Mathias LJ. Polymer 2003;44(18):5131–6.
[7] Nie J, LindéN L, Rabek JF, Fouassier JP, Morlet-Savary F, Scigalski F, et al. Acta Polymerica 1998;49(4):145–61.
[8] Sideridou I, Tserki V, Papanastasiou G. Biomaterials 2002;23(8):1819–29.
[9] Allen PEM, Clayton AB, Williams DRG. European Polymer Journal 1994;30(4):427–32.
[10] Benfarhi S, Decker C, Keller L, Zahouily K. European Polymer Journal 2004;40(3):493–501.
[11] Decker C, Keller L, Zahouily K, Benfarhi S. Polymer 2005;46(17): 6640–8.
[12] Mironi-Harpaz I, Narkis M, Siegmann A. Polymer Engineering and Science 2005;45(2):174–86.
[13] Yebassa D, Balakrishnan S, Feresenbet E, Raghavan D, Start PR, Hudson SD. Journal of Polymer Science, Part A: Polymer Chemistry 2004;42(6):1310–21.
[14] Keller L, Decker C, Zahouily K, Benfarhi S, Le Meins JM, Miehe-Brendle J. Polymer 2004;45(22):7437–47.
[15] Solomon DH, Swift JD. Journal of Applied Polymer Science 1967; 11(12):2567–75.
[16] Fu X, Qutubuddin S. Polymer Engineering and Science 2004;44(2): 345–51.
[17] Fu X, Qutubuddin S. Polymer 2001;42(2):807–13.
[18] Uhl FM, Davuluri SP, Wong SC, Webster DC. Polymer 2004;45(18): 6175–87.
[19] Wheeler PA, Wang J, Baker J, Mathias LJ. Chemistry of Materials 2005;17(11):3012–8.
[20] He H, Duchet J, Galy J, Gerard JF. Journal of Colloid and Interface Science 2005;288(1):171–6.
[21] Bauer F, GläSel HJ, Hartmann E, Bilz E, Mehnert R. Nuclear Instruments and Methods in Physics Research, Section B: Beam Interactions with Materials and Atoms 2003;208:267–70.
[22] Bauer F, Mehnert R. Journal of Polymer Research 2005;12(6):483–91.
[23] Bauer F, Ernst H, Hirsch D, Naumov S, Pelzing M, Sauerland V, et al. Macromolecular Chemistry and Physics 2004;205(12):1587–93.
[24] Decker C. Polymer International 1998;45(2):133–41.
[25] Herrera NN, Letoffe JM, Putaux JL, David L, Bourgeat-Lami E. Langmuir 2004;20(5):1564–71.
[26] Stansbury JW, Dickens SH. Dental Materials 2001;17(1):71–9.
[27] Lee TY, Guymon CA, Jönsson ES, Hoyle CE. Polymer 2004;45(18): 6155–62.
[28] Acemana S, Lahav N, Yariv S. Thermochimica Acta 1999;340–341: 349–66.
[29] Skoog DA, Leary JJ. Principles of instrumental analysis. Orlanda: Saunders College Publishing; 1992.
[30] Graessley WW. Macromolecules 1975;8:186–90.
[31] Huang NJ, Sundberg DC. Journal of Polymer Science, Part A: Polymer Chemistry 1995;33:2551–70.